

図4 動脈内径の時系列変化。a)超音波診断法を用いた計測動脈内径のBモード画像と、内径のオートトレース。b) 動脈内径の時系列曲線と心電図記録。超音波診断法により動脈の内径の時系列曲線をオートトレースし、その時系列曲線を観測すると (a)、動脈圧波形とほぼ同様の時系列曲線が得られ、心電図の R 波から、脈波伝播時間の後に、動脈の拡張が開始している(b)。すなわち、計測動脈に伝播される脈波による内径の時系列変動が、ダイレクトに脈波によって診断されていることになる。

a)



b)

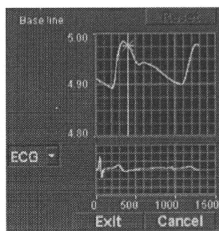


図5 東北大学病院検査室における臨床試験の一例。医学系研究科倫理委員会の審査を経た後、橈骨動脈脈波、心電図が同時記録されている。ティルトベッドに乗る被験者は大学院医学系研究科内部障害学の上月教授。

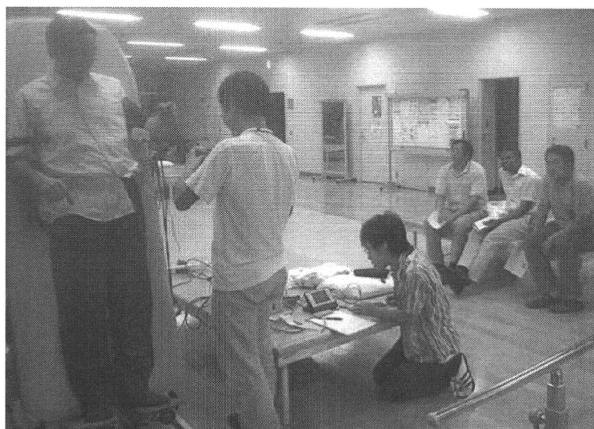


図6 心臓と動脈の血圧反射機能診断装置の検査結果の一例。被験者の心拍、血圧、脈波伝播時間の時系列と、それぞれの時系列のスペクトル解析結果。心臓と動脈の血圧反射機能の回帰直線が右下に提示されている。

Sub2-Supine

氏名: Sub2
 検査日: 2007/02/07
 FileName = PAT070207_sub2arri

[HR]
 Mean(Std) 64.9 (1.9)

[BPF]
 Mean(Std) 106.0 (5.0)
 Max/Min 137/ 65

[PTT]
 Mean(Std) 197.6 (4.3)

RR50 0.00
 CVRR 2.92
 LF/HF(HR) 2.25
 α LF 4.68
 α HF 4.29

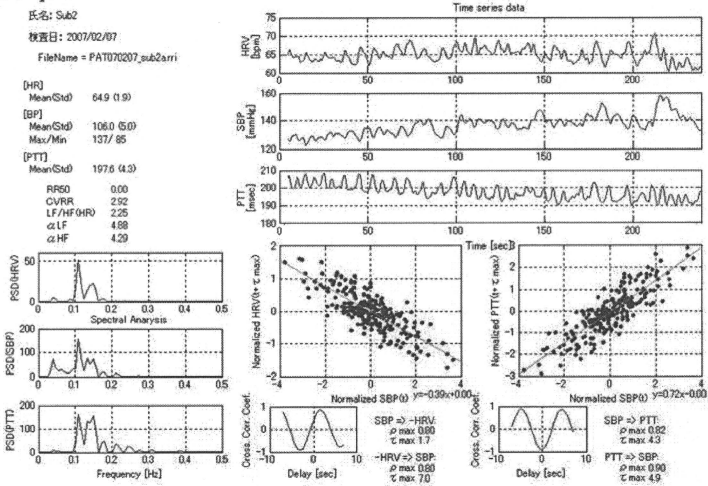


表1 自律訓練法の血行動態に与える影響

	Before	During	After
HR	66.8±9.6	67.2±8.3	66.7±9.0
BP	119.5±8.2	120.2±10.7	117.8±12.0
PTT	144.0±15.6	144.7±16.4	144.6±16.0
SV	80.9±13.4	82.1±13.4	80.3±13.8
TPR	16.0±2.2	15.8±2.3	15.7±2.5

表2 自律訓練法の血圧反射機能に与える影響

	Before	During	After
LF/HF	1.76±0.87	5.85±4.82	2.19±1.59
BP-HR	0.64±0.30	0.73±0.31	0.72±0.29
BP-PTT	0.30±0.16	0.43±0.22	0.38±0.15
BP-SV	0.22±0.02	0.02±0.01	0.02±0.01

III. 研究成果の刊行に関する一覧表

書籍

著者氏名	論文タイトル名	書籍全体の編集者名	書籍名	出版社名	出版地	出版年	ページ

雑誌

発表者氏名	論文タイトル名	発表誌名	巻号	ページ	出版年
Takayama, S., T. Seki, T. Nakazawa, N. Aizawa, S. Takahashi, M. Watanabe, M. Izumi, S. Kaneko, T. Kamiya, A. Matsuda, A. Kikuchi, T. Yambe, M. Yoshizawa, S. Nitta & N. Yaegashi	Short-term effects of acupuncture on open-angle glaucoma in retrobulbar circulation: additional therapy to standard medication.	eCAM		157090	2011
Tanaka, A., N. Sugita, M. Yoshizawa, M. Abe & T. Yambe	Dynamic characteristics between the subjective score of motion sickness discomfort and video global motion.	Conference proceedings : ... Annual International Conference of the IEEE Engineering in Medicine and Biology Society. IEEE Engineering in Medicine and Biology Society.		1368-9	2010
Sugai, T. K., A. Tanaka, M. Yoshizawa, Y. Shiraishi, T. Yambe, S. Nitta & A. Baba	Estimation of maximum ventricular elastance under assistance with a rotary blood pump.	Artificial organs	34	442-6	2010
Sugai, T. K., A. Tanaka, M. Yoshizawa, Y. Shiraishi, A. Baba, T. Yambe & S. Nitta	Influence of rotary blood pumps over preload recruitable stroke work.	Conference proceedings : ... Annual International Conference of the IEEE Engineering in Medicine and Biology Society. IEEE Engineering in Medicine and Biology Society.		2367-70	2010
Sugita, N. M. Yoshizawa, M. Murakoshi, M. Abe, N. Homma, T. Yambe & S. Nitta	Extraction of the Mayer wave component in blood pressure from the instantaneous phase difference between electrocardiograms and photoplethysmograms	Artif Life Robotics	15	522-525	2010
Yoshizawa, M., N. Sugita, S. Konno, M. Abe, A. Tanaka, T. K. Sigai, T. Yambe & S. Nitta	Assessment of effects of habitual exercise on the autonomic nervous function using plethysmogram	Conference proceedings : GCOE国際シンポジウム			2011
山家智之、金野敏、白石泰之、川島隆太、阿部恒之、杉田典夫、吉澤誠、関隆志	診断治療機能を保持する自動車の可能性	日本臨床生理学雑誌		Vol 40, NO. 1	5月14日 2010

IV. 研究成果の刊行物・別刷

Research Article

Short-Term Effects of Acupuncture on Open-Angle Glaucoma in Retrobulbar Circulation: Additional Therapy to Standard Medication

Shin Takayama,¹ Takashi Seki,¹ Toru Nakazawa,² Naoko Aizawa,² Seri Takahashi,² Masashi Watanabe,¹ Masayuki Izumi,¹ Soichiro Kaneko,¹ Tetsuharu Kamiya,¹ Ayane Matsuda,¹ Akiko Kikuchi,¹ Tomoyuki Yambe,³ Makoto Yoshizawa,⁴ Shin-ichi Nitta,³ and Nobuo Yaegashi¹

¹ Department of Traditional Asian Medicine, Graduate School of Medicine, Tohoku University,

1-1 Seiryō-machi, Aoba-ku, Sendai, Miyagi 980-8574, Japan

² Department of Ophthalmology and Visual Science, Graduate School of Medicine, Tohoku University, Sendai 980-8574, Japan

³ Institute of Development, Aging and Cancer, Tohoku University, Sendai 980-8575, Japan

⁴ Research Division on Advanced Information Technology, Cyberscience Center, Tohoku University, Japan

Correspondence should be addressed to Takashi Seki, t-seki@m.tohoku.ac.jp

Received 29 October 2010; Revised 7 December 2010; Accepted 11 January 2011

Copyright © 2011 Shin Takayama et al. This is an open access article distributed under the Creative Commons Attribution License, which permits unrestricted use, distribution, and reproduction in any medium, provided the original work is properly cited.

Background. The relation between glaucoma and retrobulbar circulation in the prognosis has been indicated. Purpose. To investigate the effects of acupuncture on retrobulbar circulation in open-angle glaucoma (OAG) patients. Methods. Eleven OAG patients (20 eyes with OAG) who were treated by topical antiglaucoma medications for at least 3 months were enrolled. Acupuncture was performed once at acupoints BL2, M-HN9, ST2, ST36, SP6, KI3, LR3, GB20, BL18, and BL23 bilaterally. Retrobulbar circulation was measured with color Doppler imaging, and intraocular pressure (IOP) was also measured at rest and one hour after rest or before and after acupuncture. Results. The α value of the resistive index in the short posterior ciliary artery ($P < .01$) and the α value of IOP ($P < .01$) were decreased significantly by acupuncture compared with no acupuncture treatment. Conclusions. Acupuncture can improve the retrobulbar circulation and IOP, which may indicate the efficacy of acupuncture for OAG.

1. Introduction

Glaucoma is one of the causes of blindness [1] and the Tajimi Study showed that the prevalence of primary open-angle glaucoma (OAG) was 3.9% in Japan [2]. The main treatment strategy of glaucoma is to control the intraocular pressure (IOP) [3]. Although IOP reduction is currently the main target for the treatment of glaucoma, treatment modalities that enhance retrobulbar hemodynamics in addition to reducing IOP may have a beneficial effect on the glaucoma therapy. It has been reported that glaucoma is associated with reduction in the blood flow velocity and elevation of the resistive index (RI) in the retrobulbar vessels [4–7]. It has also been reported that patients with OAG have impaired hemodynamics in ophthalmic circulation [8–10].

The impaired ocular circulation contributes to the progression of glaucomatous damage [11–13]. Therefore, new drugs or interventions that improve ocular hemodynamics may be preferable.

Recently, acupuncture has been widely applied to treat several conditions such as neck pain, shoulder pain, lumbar pain, headache, and hypertension in Asian and Western countries, and it has also been found to be effective for many conditions in several randomized trials [14–20]. Acupuncture has also been used for the treatment of ocular diseases, including glaucoma, in traditional Chinese medicine [21]. We have shown that acupuncture therapy added to the standard medication could affect the IOP level in eyes with normal-tension glaucoma [22], and several other studies have demonstrated that

acupuncture improves choroidal blood flow in the eye [23–25].

We have already reported that color Doppler imaging (CDI) by ultrasound is suitable for measuring the blood flow change in several organs during traditional Chinese medicine therapy [26–30]. The real-time and noninvasive hemodynamic measurement with CDI has been applied for measuring the retrolubar vessel hemodynamics, and the reproducibility has already been shown [31]. In this study, we evaluate the hemodynamic changes in retrolubar vessels by CDI to investigate the effect of acupuncture on OAG eyes.

2. Subjects

After the ethics committee approved the study, 11 patients diagnosed with OAG (20 eyes with OAG) were enrolled in this study. The patients received standard medical treatment for at least 3 months. The patients who had an experience of laser trabeculoplasty, any ocular surgery, or inflammation within the past year were excluded in the present study.

3. Methods

3.1. Acupuncture. On the trial days, the patients arrived under regular medications. They received acupuncture therapy as follows in the morning. The acupoints were selected on the basis of the principles of traditional Chinese medicine. Acupuncture was performed for 15 min using disposable stainless steel needles (0.16 mm or 0.20 mm × 40 mm; Seirin Co. Ltd., Shizuoka, Japan) at acupoints Cuanzhu (BL2), Taiyang (M-HN9), Sibai (ST2), Zusanli (ST36), Sanyinjiao (SP6), Taixi (KI3), and Taichong (LR3) bilaterally while the patient was in the supine position and at acupoints Fengchi (GB20), Ganshu (BL18), and Shenshu (BL23) bilaterally while the patient was in the prone position for 15 min. Each needle was simply inserted without any intention of eliciting specific responses (e.g., de-qi feelings) to a depth of approximately 20 mm at acupoints ST36, SP6, KI3, GB20, BL18, and BL23. For acupoints BL2, M-HN9, ST2, and LR3, the needles were inserted to a depth of approximately 3–10 mm. Neither needle manipulation techniques nor other auxiliary interventions were used. Five licensed acupuncturists and one physician-acupuncturist with over 5 years of acupuncture experience administered the acupuncture treatment.

3.2. Measurements. To minimize the effects of diurnal variation, all measurements were recorded at the same time of the day (between 10 AM and 11 AM) for each patient by the same examiner. As a control, the subjects received the measurements of the systemic hemodynamics, retrolubar vessel hemodynamics, and IOP that were performed at rest and one hour after rest. One month later, they received the same measurements before and after acupuncture treatment. The systemic hemodynamics was measured by an oscillometer and the hemodynamics in retrolubar vessels was measured by ultrasound (LOGIQ e, GE Healthcare, Tokyo, Japan). The ultrasound measurements were performed after 10-minute

Table 1: Characteristic data of the patients with open-angle glaucoma.

Variable	Value
Number of patients	11
Age (years)	63 • 11
Sexuality (male, female)	(1, 10)
Number of eyes with glaucoma	20
Best corrected visual acuity	1.1 • 0.3
Spherical equivalent (D)	• 1.6 • 3.2
Humphrey automated perimeter	
Mean deviation (dB)	• 11.5 • 7.8
Pattern standard deviation (dB)	10.2 • 4.5
OCT RNFL thickness (µm)	70.5 • 21.8
The number of topical medications	
None	1
One kind	4
Two kinds	1
More than three kinds	5

rest in an air-conditioned room, avoiding any pressure on the eye, with the patients in the supine position. CDI was performed with a 13 MHz linear transducer for retrolubar vessels such as the ophthalmic artery (OA), central retinal artery (CRA), and short posterior ciliary artery (SPCA). The OA was examined approximately 20 mm behind the globe (Figure 1(a)), the CRA was examined within 5 mm of the retrolaminar portion of the optic nerve (Figure 1(b)), and the temporal SPCA was examined approximately 5–10 mm behind the globe (Figure 1(c)). All blood flow velocity waveforms were measured at the corrected Doppler angle. Resistive index (RI: (peak systolic velocity • end-diastolic velocity)/peak systolic velocity) was also measured in each retrolubar vessel.

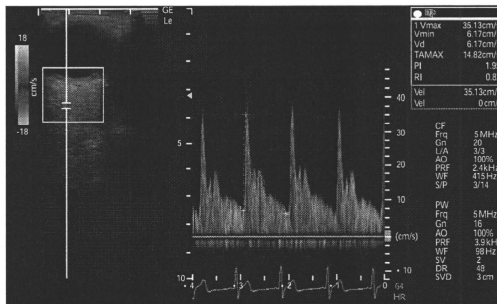
3.3. Statistical Analysis. Statistical analysis was performed with the SPSS software (version 16.0, SPSS Japan Inc., Tokyo, Japan). The parameters between before and after acupuncture or between control and acupuncture were compared by paired t-test.

4. Results

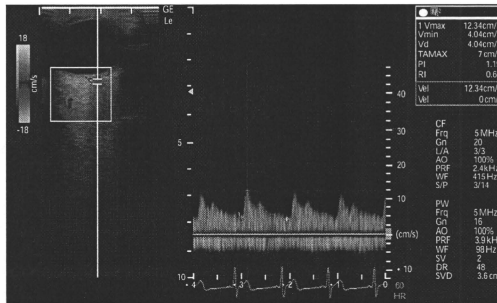
Table 1 shows the characteristics of the subjects. One male and ten female glaucoma patients with a mean age of 63 • 11 years were observed. The systemic hemodynamic parameters including heart rate, blood pressure, and IOP are shown in Table 2. The blood pressure and heart rate did not change significantly by acupuncture.

The IOP level significantly decreased by acupuncture compared with before acupuncture ($P < .05$). The • value of IOP also significantly decreased by acupuncture compared with control ($P < .01$) (Table 2).

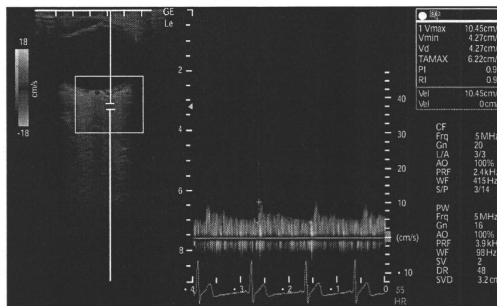
Retrolubar vessel RI in the OA, CRA, and SPCA is shown in Table 3. The RI in the CRA and SPCA decreased



(a)



(b)



(c)

Figure 1: Horizontal scans by color Doppler imaging through the globe showing the (a) ophthalmic artery, (b) central retinal artery, and (c) short posterior ciliary artery.

Table 2: Blood pressure, heart rate, and intraocular pressure in control and acupuncture therapy. The values represent the mean and SD. * P < .05, ** P < .01 versus rest or before acupuncture. * P < .05, ** P < .01 versus control.

Parameter	Control		• value	Acupuncture		• value
	Rest	After 1 hour		Before	After	
Systole blood pressure (mm Hg)	116.4 • 10.0	119.8 • 7.6	3.4 • 7.4	124.5 • 12.9	122.6 • 9.7	• 1.1 • 7.9
Diastolic blood pressure (mm Hg)	69.8 • 6.5	68.6 • 3.9	• 1.0 • 9.4	74.5 • 5.4	72.0 • 2.9	• 3.0 • 5.5
Heart rate (beats/min)	61.5 • 7.3	60.1 • 8.1	• 2.5 • 3.8	61.7 • 8.5	60.3 • 10.4	• 2.4 • 5.5
Intraocular pressure (mm Hg)	16.0 • 4.1	17.1 • 4.2*	1 • 0.9	17.0 • 5.0	16.0 • 4.3*	• 1 • 1.9**

Table 3: Resistive index (RI) in the ophthalmic artery, central retinal artery, and short posterior ciliary artery. The values represent the mean and SD. * P < .05, ** P < .01 versus before acupuncture. * P < .05, ** P < .01 versus control.

Resistive index	Control		• value	Acupuncture		• value
	Rest	After 1 hour		Before	After	
Ophthalmic artery	0.74 • 0.04	0.75 • 0.05	0.006 • 0.037	0.74 • 0.04	0.74 • 0.04	• 0.006 • 0.036
Central retinal artery	0.75 • 0.09	0.72 • 0.03	• 0.027 • 0.085	0.72 • 0.05	0.68 • 0.04*	• 0.036 • 0.059
Short posterior ciliary artery	0.68 • 0.05	0.68 • 0.04	0.004 • 0.038	0.67 • 0.04	0.64 • 0.06*	• 0.032 • 0.054**

significantly by acupuncture compared with before acupuncture (P < .05). The • value of RI in the SPCA also significantly decreased by acupuncture compared with control (P < .01) (Table 3).

5. Discussion

To our best knowledge, this is the first report on hemodynamic change in retrobulbar vessels related to acupuncture in OAG eyes. The present findings suggest that acupuncture can alter vessel resistance in the SPCA, even though the eyes are treated with standard medications.

The OA originates from the internal carotid artery. The CRA and SPCA are the ocular branches of the OA [32]. The CRA supplies blood to the retina and SPCA, to the choroid. CDI by ultrasound is useful for the measurement of the blood flow in various vessels in real time. Since it is impossible to determine the diameter of very small retrobulbar vessels, CDI cannot directly measure blood flow volume. However, the decrease of the distal vascular resistance in the SPCA indicates an increase of the blood flow in the choroid. We have already reported that acupuncture could increase the blood flow volume in the upper limb without an increase in the cardiac output, and the increased reaction in the blood flow was mediated by the decrease in the vascular resistance on the basis of the decreased vascular tone [30]. The mechanisms by which acupuncture can alter retrobulbar vessel circulation are still unclear. However, it has been reported that the blood flow in the eye is controlled by sympathetic and parasympathetic nerves, and it is related with the release of nitric oxide or calcitonin gene-related peptide [33, 34]; it has also been reported that the regulation of regional blood flow by somatic afferent stimulation is based on somatoautonomic reflex mechanisms in the choroidal blood flow of the eyeball [34]. The hemodynamic changes in the SPCA by acupuncture may be related with these mechanisms. Reduced blood flow velocities and increased vascular resistance in the retrobulbar

arteries appear to be a risk factor for glaucoma progression [35–38]. Thus, acupuncture may be applied for additional therapy to treat OAG.

We should view these results cautiously because the present study was a case series study and intervention was provided only once. Longer observation of acupuncture therapy is needed to investigate the progression of glaucomatous damage associated with impaired ocular circulation.

6. Conclusions

The vessel resistance in the SPCA and the IOP level were decreased by acupuncture in OAG eyes. Acupuncture can affect the retrobulbar circulation and IOP despite the administration of standard medication. The present study implies the possibility that acupuncture is effective for OAG with standard medication.

Acknowledgment

This work was supported by Health and Labour Sciences Research Grants for Clinical Research from the Japanese Ministry of Health, Labour and Welfare.

References

- [1] K. Nakae, K. Masuda, T. Aneo et al., "Wagakuni ni okeru shiryokushougai no genjū," Research Committee on Chorioretinal Degenerations and Optic Atrophy, the Ministry of Health, Labour and Welfare of Japan, vol. 17, pp. 263–276, 2005.
- [2] A. Iwase, Y. Suzuki, M. Araie et al., "The prevalence of primary open-angle glaucoma in Japanese: the Tajimi study," *Ophthalmology*, vol. 111, no. 9, pp. 1641–1648, 2004.
- [3] R. N. Weinreb and P. Tee Khaw, "Primary open-angle glaucoma," *The Lancet*, vol. 363, no. 9422, pp. 1711–1720, 2004.
- [4] C. Akarsu and M. Y. K. Bilgili, "Color Doppler imaging in ocular hypertension and open-angle glaucoma," *Graefes*

- Archive for Clinical and Experimental Ophthalmology, vol. 242, no. 2, pp. 125–129, 2004.
- [5] V. P. Costa, A. Harris, E. Stefánsson et al., "The effects of anti-glaucoma and systemic medications on ocular blood flow," *Progress in Retinal and Eye Research*, vol. 22, no. 6, pp. 769–805, 2003.
 - [6] H. J. Kaiser, A. Schoetzau, D. Stumpfing, and J. Flammer, "Blood-flow velocities of the extraocular vessels in patients with high-tension and normal-tension primary open-angle glaucoma," *American Journal of Ophthalmology*, vol. 123, no. 3, pp. 320–327, 1997.
 - [7] S. J. A. Rankin, "Color Doppler imaging of the retrobulbar circulation in glaucoma," *Survey of Ophthalmology*, vol. 43, no. 1, pp. S176–S182, 1999.
 - [8] I. Stalmans, A. Harris, S. Fieuews et al., "Color Doppler imaging and ocular pulse amplitude in glaucomatous and healthy eyes," *European Journal of Ophthalmology*, vol. 19, no. 4, pp. 580–587, 2009.
 - [9] I. Janulevičienė, I. Sliesoraitytė, B. Siesky, and A. Harris, "Diagnostic compatibility of structural and haemodynamic parameters in open-angle glaucoma patients," *Acta Ophthalmologica*, vol. 86, no. 5, pp. 552–557, 2008.
 - [10] N. Plange, M. Kaup, O. Arend, and A. Remky, "Asymmetric visual field loss and retrobulbar haemodynamics in primary open-angle glaucoma," *Graefes Archive for Clinical and Experimental Ophthalmology*, vol. 244, no. 8, pp. 978–983, 2006.
 - [11] M. Satilmis, S. Orgül, B. Doubler, and J. Flammer, "Rate of progression of glaucoma correlates with retrobulbar circulation and intraocular pressure," *American Journal of Ophthalmology*, vol. 135, no. 5, pp. 664–669, 2003.
 - [12] J. Schumann, S. Orgül, K. Gugleta, B. Dubler, and J. Flammer, "Intercocular differences in progression of glaucoma correlates with interocular differences in retrobulbar circulation," *American Journal of Ophthalmology*, vol. 129, no. 6, pp. 728–733, 2000.
 - [13] Y. Yamazaki and S. M. Drance, "The relationship between progression of visual field defects and retrobulbar circulation in patients with glaucoma," *American Journal of Ophthalmology*, vol. 124, no. 3, pp. 287–295, 1997.
 - [14] X. Xu, "Acupuncture in an outpatient clinic in China: a comparison with the use of acupuncture in North America," *Southern Medical Journal*, vol. 94, no. 1-10, pp. 813–816, 2001.
 - [15] V. Napadow and T. J. Kaptchuk, "Patient characteristics for outpatient acupuncture in Beijing, China," *Journal of Alternative and Complementary Medicine*, vol. 10, no. 3, pp. 565–572, 2004.
 - [16] C. M. Witt, S. Jena, B. Brinkhaus, B. Liecker, K. Wegscheider, and S. N. Willich, "Acupuncture for patients with chronic neck pain," *Pain*, vol. 125, no. 1-2, pp. 98–106, 2006.
 - [17] B. Brinkhaus, C. M. Witt, S. Jena et al., "Acupuncture in patients with chronic low back pain: a randomized controlled trial," *Archives of Internal Medicine*, vol. 166, no. 4, pp. 450–457, 2006.
 - [18] D. Melchart, A. Streng, A. Hoppe et al., "Acupuncture in patients with tension-type headache: randomised controlled trial," *British Medical Journal*, vol. 331, no. 7513, pp. 376–379, 2005.
 - [19] C. Witt, B. Brinkhaus, S. Jena et al., "Acupuncture in patients with osteoarthritis of the knee: a randomised trial," *The Lancet*, vol. 366, no. 9480, pp. 136–143, 2005.
 - [20] K. Linde, A. Streng, S. Jürgens et al., "Acupuncture for patients with migraine: a randomized controlled trial," *Journal of the American Medical Association*, vol. 293, no. 17, pp. 2118–2125, 2005.
 - [21] *Diseases of Eyes, Ears, Nose and Throat*, vol. 681, Eastland Press, Seattle, Wash. USA, 1981.
 - [22] M. Kuruusu, K. Watanabe, T. Nakazawa et al., "Acupuncture For Patients With Glaucoma," *Explore*, vol. 1, no. 5, pp. 372–376, 2005.
 - [23] S. Naruse, K. Mori, M. Kurihara et al., "Chorioretinal blood flow changes following acupuncture between thumb and forefinger," *Journal of Japanese Ophthalmological Society*, vol. 104, no. 10, pp. 717–723, 2000.
 - [24] M. Shimura, S. Uchida, A. Suzuki, K. Nakajima, and Y. Aikawa, "Reflex choroidal blood flow responses of the eyeball following somatic sensory stimulation in rats," *Autonomic Neuroscience*, vol. 97, no. 1, pp. 35–41, 2002.
 - [25] J. J. Steinle, D. Krizsan-Agbas, and P. G. Smith, "Regional regulation of choroidal blood flow by autonomic innervation in the rat," *American Journal of Physiology*, vol. 279, no. 1, pp. R202–R209, 2000.
 - [26] S. Takayama, T. Seki, N. Sugita et al., "Radial artery hemodynamic changes related to acupuncture," *Explore*, vol. 6, no. 2, pp. 100–105, 2010.
 - [27] S. Takayama, T. Seki, M. Watanabe et al., "Changes of blood flow volume in the superior mesenteric artery and brachial artery with abdominal thermal stimulation," *Evidence-Based Complementary and Alternative Medicine*, vol. 17, pp. 1–9, 2009.
 - [28] S. Takayama, T. Seki, M. Watanabe et al., "The herbal medicine Daikenchuto increases blood flow in the superior mesenteric artery," *Tohoku Journal of Experimental Medicine*, vol. 219, no. 4, pp. 319–330, 2009.
 - [29] S. Takayama, T. Seki, M. Watanabe et al., "The effect of warming of the abdomen and of herbal medicine on superior mesenteric artery blood flow—a pilot study," *Forschende Komplementärmedizin*, vol. 17, no. 4, pp. 195–201, 2010.
 - [30] S. Takayama, T. Seki, M. Watanabe et al., "Brief effect of acupuncture on the peripheral arterial system of the upper limb and systemic hemodynamics in humans," *Journal of Alternative and Complementary Medicine*, vol. 16, no. 7, pp. 707–713, 2010.
 - [31] E. T. Matthiessen, O. Zeitz, G. Richard, and M. Klemm, "Reproducibility of blood flow velocity measurements using colour decoded Doppler imaging," *Eye*, vol. 18, no. 4, pp. 400–405, 2004.
 - [32] S. S. Hayreh and R. Dass, "The ophthalmic artery II: intra orbital course," *The British Journal of Ophthalmology*, vol. 46, no. 3, pp. 165–185, 1962.
 - [33] A. K. Wiencke, H. Nilsson, P. J. Nielsen, and N. C. B. Nyborg, "Nonadrenergic noncholinergic vasodilation in bovine ciliary artery involves CGRP and neurogenic nitric oxide," *Investigative Ophthalmology and Visual Science*, vol. 35, no. 8, pp. 3268–3277, 1994.
 - [34] M. Shimura, S. Uchida, A. Suzuki, K. Nakajima, and Y. Aikawa, "Reflex choroidal blood flow responses of the eyeball following somatic sensory stimulation in rats," *Autonomic Neuroscience*, vol. 97, no. 1, pp. 35–41, 2002.
 - [35] D. Gherghel, S. Orgül, K. Gugleta, M. Gekkieva, and J. Flammer, "Relationship between ocular perfusion pressure and retrobulbar blood flow in patients with glaucoma with progressive damage," *American Journal of Ophthalmology*, vol. 130, no. 5, pp. 597–605, 2000.
 - [36] O. Zeitz, P. Galambos, L. Wagenfeld et al., "Glaucoma progression is associated with decreased blood flow velocities in the short posterior ciliary artery," *British Journal of Ophthalmology*, vol. 90, no. 10, pp. 1245–1248, 2006.

- [37] F. Galassi, A. Sodi, F. Ucci, G. Renieri, B. Pieri, and M. Baccini, "Ocular hemodynamics and glaucoma prognosis: a color Doppler imaging study," *Archives of Ophthalmology*, vol. 121, no. 12, pp. 1711–1715, 2003.
- [38] A. Martínez and M. Sánchez, "Predictive value of colour Doppler imaging in a prospective study of visual field progression in primary open-angle glaucoma," *Acta Ophthalmologica Scandinavica*, vol. 83, no. 6, pp. 716–722, 2005.

ORIGINAL ARTICLE

Norihiro Sugita · Makoto Yoshizawa
Masayuki Murakoshi · Makoto Abe · Noriyasu Homma
Tomoyuki Yambe · Shin-ichi Nitta

Extraction of the Mayer wave component in blood pressure from the instantaneous phase difference between electrocardiograms and photoplethysmograms

Received and accepted: August 11, 2010

Abstract To analyze the human baroreflex function non-invasively, a beat-by-beat blood pressure signal is often measured by tonometry or plethysmogram using continuous blood pressure sensors. However, these sensors are too expensive and bulky to be used for home healthcare or telemedicine. On the other hand, it is well known that the pulse transmission time (PTT) is strongly correlated with the beat-by-beat blood pressure, especially in the Mayer wave-related frequency band (0.05–0.15 Hz). To obtain a new physiological parameter with a higher correlation with blood pressure in this band compared with that obtained using the PTT alone, we proposed the same-phase temporal difference (SPTD) based on electrocardiogram and photoplethysmogram signals. By examining 94 healthy subjects using a combination of SPTD and conventional PTT, it was revealed that the correlation with blood pressure for 25 subjects could be improved using the SPTD instead of the PTT, by applying the criterion of the ratio of their powers. However, for 7 subjects, the correlation decreased.

Key words Blood pressure · Pulse transmission time · Instantaneous phase · Photoplethysmogram

1 Introduction

Escalating medical costs caused by rapid aging of the population, and health disparities caused by a shortage of physi-

cians, are serious problems in Japan. Telemedicine could be a viable solution to these problems. For telemedicine to be functional, however, doctors require physiological information such as the electrocardiograms (ECG) and blood pressure of patients in remote places.

In this study, we focused on the baroreflex system as a new physiological information source for telemedicine. The baroreflex system is a negative feedback control mechanism in the autonomic nervous system that can attenuate the effects of perturbations in arterial blood pressure by changing the heart rate or vascular resistance; cardiovascular diseases such as hypertension are associated with malfunctions of this system.^{1,4}

To estimate the baroreflex characteristics, a beat-by-beat blood pressure signal is frequently measured by tonometry or plethysmogram using continuous blood pressure sensors. However, these sensors are too expensive and bulky to be used for home healthcare or telemedicine. On the other hand, it is well known that the pulse transmission time, or pulse transit time (PTT), is strongly correlated with the beat-by-beat blood pressure,⁵ especially in the so-called Mayer wave-related frequency band (0.05–0.15 Hz). To obtain a more accurate PTT signal in the Mayer wave-related band instead of blood pressure, this study proposes a new algorithm based on the instantaneous phase difference between ECG and photoplethysmograms (PPG).

As shown in Fig. 1, the PTT is defined as the time delay between the R-wave in the ECG and the pulse arrival at a peripheral point, for example, at a finger tip. Therefore, the accuracy of PTT depends on how these time points are detected. Most conventional methods use the moment when the finger PPG signal begins to rise after the R-wave appears as the arrival time. However, the arrival time obtained from a PPG is easily disturbed by noise and artifacts. There are several methods to detect the arrival time,⁶ but it is not clear which is the most appropriate method for calculating the PTT. In this study, we propose a new method for calculating the PTT on the basis of the instantaneous phase difference between the ECG and PPG waves. The results are compared with those of the conventional method.

N. Sugita (✉) · M. Yoshizawa · M. Abe · N. Homma
Cybercience Center, Tohoku University, 6-6-05 Aoba, Aramaki,
Aoba-ku, Sendai 980-8579, Japan
e-mail: sugita@yoshizawa.ceci.tohoku.ac.jp

M. Murakoshi
Graduate School of Biomedical Engineering, Tohoku University,
Sendai, Japan

T. Yambe · S. Nitta
Institute of Development, Aging and Cancer, Tohoku University,
Sendai, Japan

This work was presented in part at the 15th International Symposium on Artificial Life and Robotics, Oita, Japan, February 4–6, 2010

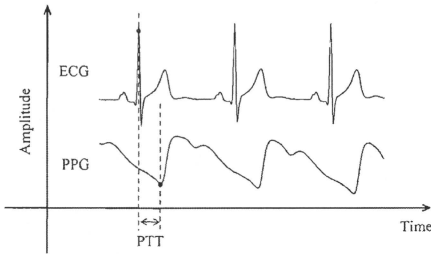


Fig. 1. Definition of pulse transmission time (PTT)

2 Methods

2.1 Same-phase temporal difference

As a new index for determining the PTT, we propose the same-phase temporal difference (SPTD) between the ECG and PPG signals, as follows.

Suppose that a biological signal $s(t)$ at time t is given by

$$s(t) = \sum_k C_k \cos \theta_k(t) \quad (1)$$

$$\theta_k(t) = k\omega_0 t + \psi_k + \phi_k(t) \quad (2)$$

where C_k , ψ_k , and $\phi_k(t)$ are a Fourier coefficient, an initial phase, and an instantaneous phase of the k -th harmonic wave, respectively, and ω_0 is a base angular frequency. If $k = 1$ and $t = t_m$, which is the time of the appearance of a feature point (e.g., the peak of an ECG R-wave) at the m -th beat, Eq. 2 is represented by

$$\theta_1(t_m) = \omega_0 t_m + \psi_1 + \phi_1(t_m) = 2m\pi \quad (3)$$

So the time interval TI_m between the feature point at the m -th beat and that at the $(m+1)$ -th beat is given by

$$TI_m = \theta_1^{-1}(2(m+1)\pi) - \theta_1^{-1}(2m\pi) \quad (4)$$

where $\theta_1^{-1}(\bullet)$ is the inverse function of $\theta_1(\bullet)$. Here, suppose that $s(t)$ is an ECG signal. Then TI_m indicates the R-R interval at the m -th beat. In the same way, if $s(t)$ is a PPG signal, TI_m is the heartbeat interval obtained from the PPG signal.

The PTT is considered to be the time interval between the feature point on the ECG and that on the PPG at the same beat. The SPTD at the m -th beat, $SPTD_m$, is defined as

$$SPTD_m = \theta_{\text{ECG}}^{-1}(2m\pi) - \theta_{\text{PPG}}^{-1}(2m\pi) \quad (5)$$

where $\theta_{\text{ECG}}^{-1}(2m\pi)$ and $\theta_{\text{PPG}}^{-1}(2m\pi)$ are the inverse functions of the corresponding phase function shown in Eq. 3 when $s(t)$ is the ECG and PPG, respectively. $SPTD_m$ can be regarded as the temporal difference between the fundamental harmonics of the ECG and PPG signals.

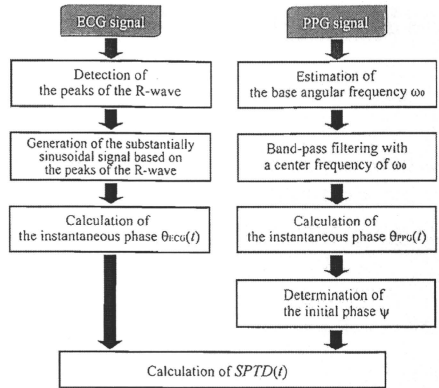


Fig. 2. Flowchart of the calculation of SPTD

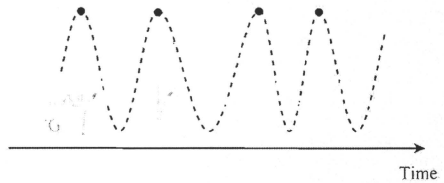


Fig. 3. Substantially sinusoidal signal whose crests appeared at the time points of R-wave peaks

2.2 Calculation method

Figure 2 shows a flowchart of the SPTD calculation. R-waves in the ECG were detected, and a substantially sinusoidal signal whose crests appeared at time points of the R-wave peaks was generated, as shown in Fig. 3. The base angular frequency ω_0 of the PPG was obtained as the peak frequency in the range 0.3–2.0 Hz. A 5th-order Butterworth band-pass filter with a center frequency of ω_0 and a bandwidth of 0.3 Hz was applied to the PPG signal. After these processes, the time series of the instantaneous phases $\theta_{\text{ECG}}(t)$ and $\theta_{\text{PPG}}(t)$ were calculated using the Hilbert transform. The initial phase of $\theta_{\text{PPG}}(t)$, $\psi_{1,\text{PPG}}$, was set to minimize the difference in the mean value between the SPTD and the conventional PTT, in which the PTT was obtained as the delay between the peak of the R-wave and the rise time of the PPG. Finally, the time series of the SPTD was given by

$$SPTD(t) = \theta_{\text{ECG}}^{-1}[\theta_{\text{PPG}}(t)] - t \quad (6)$$

Furthermore, the maximum cross-correlation coefficient R_{max} between the PTT variability and blood pressure variability, whose frequency components were limited to the

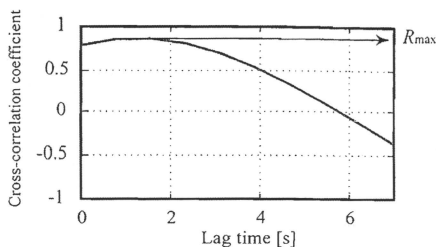


Fig. 4. Definition of the maximum cross-correlation coefficient R_{max} between two parameters

Mayer wave-related band, was defined as shown in Fig. 4. It is possible to investigate the correlation between two physiological parameters in considering of their lags by introducing R_{max} . In this study, R_{max} between the conventional PTT ($-cPTT$) and the mean blood pressure (MBP), $R_{cPTT-MBP}$, and that between $-SPTD$ and MBP , $R_{SPTD-MBP}$, were calculated. The minus sign was introduced as $-cPTT$ and $-SPTD$ because these parameters are negatively correlated with MBP .

2.3 Data acquisition

Physiological data were acquired from 94 healthy adults (69 males and 25 females, aged 23.4 ± 2.61 years). Informed consent was obtained from all subjects before the experiment. Each test subject was instructed to sit on a chair for 5 min, and their ECG and PPG were measured by electrodes placed on their chest and a photoplethysmographic sensor attached to a finger tip. The continuous arterial blood pressure signal was measured non-invasively using a finger blood pressure cuff (Portapres-Model 2; TNO-TPD Biomedical Instrumentation) or a tonometric pressure sensor (JENTOW 7700; Nihon Corin). These signals were amplified and converted to digital data by a 16-bit A/D converter (MP100; BIOPAC System). The sampling frequency was 1 kHz.

3 Results and discussion

Figure 5 shows changes in the Mayer wave component of a subject's $cPTT$ and $SPTD$. As shown in this figure, these changes were very similar.

Figure 6 shows the scatter diagram for $R_{cPTT-MBP}$ and $R_{SPTD-MBP}$. In this figure, a dot above the diagonal dashed line represents a subject whose $SPTD$ has a higher correlation with MBP than the $cPTT$ does. This result indicates that the information of the $SPTD$ is different from that of the $cPTT$, and that to get the highest possible correlation with blood pressure for some subjects, we should use $SPTD$ instead of $cPTT$. To do this, we need a criterion for determining whether

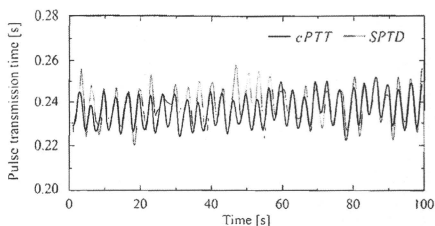


Fig. 5. Changes in the Mayer wave component of the $cPTT$ and $SPTD$ of a subject

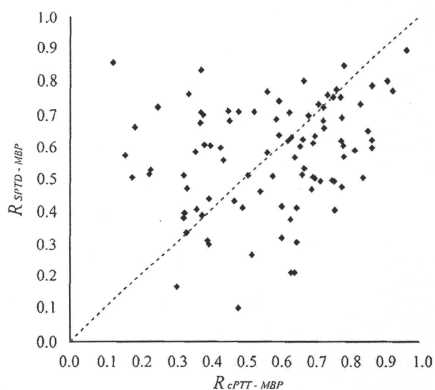


Fig. 6. Scatter diagram of $R_{SPTD-MBP}$ versus $R_{cPTT-MBP}$

to adopt $SPTD$ instead of $cPTT$ without measuring the blood pressure. For this purpose, we introduced the power ratio (PR) of $SPTD$ to $cPTT$. The index PR is defined as

$$PR = \sqrt{\frac{PW_{SPTD}}{PW_{cPTT}}} \quad (7)$$

where PW_{SPTD} and PW_{cPTT} are the powers of $SPTD$ and $cPTT$ in the Mayer wave-related band, respectively. Figure 7 shows the scatter diagram of the difference value between $R_{SPTD-MBP}$ and $R_{cPTT-MBP}$ versus the PR . This figure indicates that the difference between the two maximum cross-correlations R_{max} increases as PR increases, and that $R_{SPTD-MBP}$ is higher than $R_{cPTT-MBP}$ in most subjects whose PR is larger than 3. Thus, a new index $nPTT$ is defined as

$$nPTT = \begin{cases} SPTD & \text{if } PR \geq 3 \\ cPTT & \text{otherwise} \end{cases} \quad (8)$$

The scatter diagram of $R_{nPTT-MBP}$, which is the maximum cross-correlation between $-nPTT$ and MBP , versus $R_{cPTT-MBP}$ is shown in Fig. 8. This result shows that using $SPTD$ instead

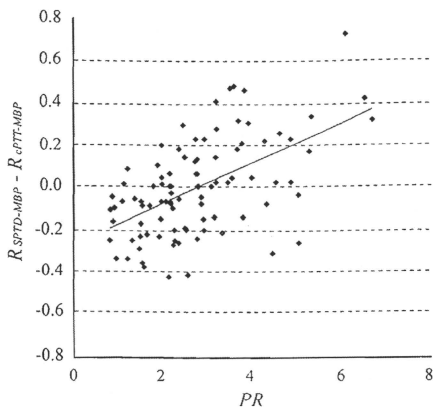


Fig. 7. Scatter diagram of the difference value between $R_{SPTD-MBP}$ and $R_{cPTT-MBP}$ versus PR . PR is the power ratio of $SPTD$ to $cPTT$ in the Mayer wave-related band

of $cPTT$ increased the value of $R_{cPTT-MBP}$ for 25 subjects (placed above the dashed line), whereas this value decreased for 7 subjects (placed below the dashed line).

The accuracy of detecting the position at which the pulse wave begins to rise is important for estimating $cPTT$. Thus, noise contamination in the PPG signal, especially around these rising points, significantly reduces the accuracy of $cPTT$. On the other hand, the result shown in Fig. 8 suggests that $SPTD$ is more robust against short-term noise and artifacts in the PPG than $cPTT$, because $SPTD$ can be calculated on the basis of a global pattern of the PPG waveform.

4 Conclusions

In this study, we focused on the pulse transmission time (PTT), as a parameter containing information about blood pressure, to use in estimating the baroreflex characteristics without measuring a continuous blood pressure signal. To obtain a new parameter with a higher correlation with blood pressure in the Mayer wave-related band, rather than using the PTT only, we proposed the same-phase temporal difference (SPTD) based on ECG and PPG signals. Experiment on 94 healthy subjects using the combination of the SPTD and conventional PTT revealed that the correlation with blood pressure for 25 subjects could be improved by

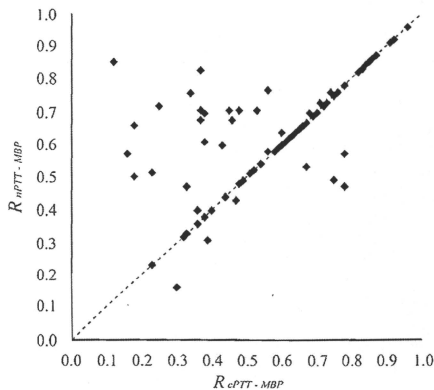


Fig. 8. Scatter diagram of $R_{SPTD-MBP}$ versus $R_{cPTT-MBP}$. $cPTT$ was selected from $cPTT$ or $SPTD$ on the basis of the PR value

using the SPTD instead of the PTT, by applying the criterion of the ratio of their powers. However, the correlation decreased for 7 subjects.

In future work, we will calculate the baroreflex characteristics using the proposed parameter to confirm its validity. Furthermore, we will investigate why the correlation decreased in some cases. This investigation could lead to the development of an alternative method for extracting information with a higher correlation with blood pressure from the ECG and PPG signals.

References

- Guo GB, Abboud FM (1984) Impaired central mediation of the arterial baroreflex in chronic renal hypertension. *Am J Physiol Heart Circ Physiol* 246:720-727
- Guido G, Bianca MC, Gino S, et al (1998) Baroreflex control of sympathetic nerve activity in essential and secondary hypertension. *Hypertension* 31:68-72
- Parati G, Rienzo MD, Bertinieri G, et al (1988) Evaluation of the baroreceptor-heart rate reflex by 24-hour intra-arterial blood pressure monitoring in humans. *Hypertension* 12:214-222
- Mancia G, Ludbrook J, Ferrari A, et al (1978) Baroreceptor reflexes in human hypertension. *Circ Res* 43:170-177
- Chen W, Kobayashi T, Ichikawa Y, et al (2000) Continuous estimation of systolic blood pressure using the pulse arrival time and intermittent calibration. *Med Biol Eng Comput* 39(8):569-574
- Kazanavicius E, Gircys R, Vrubliauskas A, et al (2005) Mathematical methods for determining the foot point of the arterial pulse wave and evaluation of proposed methods. *Info Tech Cont* 34(1):29-36



Estimation of Maximum Ventricular Elastance Under Assistance With a Rotary Blood Pump

**Telma K. Sugai, †Akira Tanaka,
‡Makoto Yoshizawa, §Yasuyuki Shiraishi,
§Tomoyuki Yambe, §Shin-ichi Nitta,
and ¶Atsushi Baba*

**Graduate School of Biomedical Engineering,
Tohoku University; ‡Cybercience Center, Tohoku
University; §Institute of Development, Aging and
Cancer, Tohoku University, Sendai; †Faculty of
Symbiotic Systems Science, Fukushima University,
Fukushima and ¶Faculty of Systems Engineering,
Shibaura Institute of Technology, Saitama, Japan*

Abstract: The maximum ventricular elastance is a reliable index for assessing the cardiac function from changes in its pressure-volume relationship. The advantage of this index is that it can represent the contractility of either unassisted hearts or native hearts assisted with rotary blood pumps. However, there are situations in which changes in the ventricular load required for the conventional estimation method might be risky. For example, in a bridge-to-recovery the cardiac function should also be continuously

doi:10.1111/j.1525-1594.2009.00876.x

Received July 2008; revised June 2009.

Address correspondence and reprint requests to Ms. Telma K. Sugai, Graduate School of Biomedical Engineering, Tohoku University, Yoshizawa Laboratory, Electrical Engineering Building, 6-6-05 Aoba, Aramaki, Aoba-ku, Sendai 980-8579, Japan. E-mail: telma@yoshizawa.ecei.tohoku.ac.jp

observed after the implantation of a rotary blood pump. In this article, we present the results of the estimation of the maximum elastance with *in vivo* data using the parameter optimization method, which is a single-beat estimation method. The estimated values for the normal cardiac function (6.8 ± 0.6 , 4.5 ± 0.9 , 4.2 ± 1.8 mm Hg/mL) were significantly different from those for the low cardiac function (3.2 ± 1.5 , 1.9 ± 1.0 , 1.9 ± 1.2 mm Hg/mL) from the data of the three animals that were analyzed. Besides, the maximum elastance values were independent of the pump rotational speed. These results indicate that this index might be useful for the detection of the myocardial recovery. **Key Words:** Elastance—Estimation techniques—Heart contractility—Myocardial recovery—Ventricular assist device—Ventricular function.

Rotary blood pumps (RBPs) have been used as bridge-to-transplantation or as destination therapy for a relatively long period, and lately have also been used as bridge-to-recovery. In the latter case, the RBP unloads the native heart while the myocardial repair is carried out by pharmacological treatments or cell therapy. The RBP is then withdrawn when sufficient recovery of cardiac function is detected. Since the withdrawal and the reimplantation, in particular, of the RBP are invasive procedures, this recovery must be closely monitored before the weaning of the RBP (1).

Currently, in order to observe the recovery of the cardiac function, the pump must be temporarily stopped (1) so that the physiologist can analyze the myocardial response. Although the off-pump tests are accurate, stopping the pump is a risky procedure, during which there can be thrombi formation or insufficient blood perfusion in peripheral tissues. Thus, a safer technique for assessment of the cardiac function is necessary.

Many indices have been used to detect the function of the unassisted native heart, such as the ejection fraction (EF), the dP/dt_{max} and the maximum ventricular elastance (E_{max}). However, the RBP changes the hemodynamics of the cardiovascular system. Therefore, it is important to verify the validity of such indices during the assistance with RBPs.

The main objective of this study was to evaluate the validity of cardiac function indices during the assistance with RBPs. In particular, we choose the E_{max} to be analyzed as it represents the ventricular contractility independently of the load (2-4), which was expected to compensate for the changes brought by different assistance conditions. In order to avoid sudden and unsuitable changes of the ventricular load that are required for the conventional multiple-beats estimation method, we present an evaluation for the estimation of E_{max} using the parameter optimization method (POM), a single beat estimation

method (5). As the gold standard, the E_{max} was also estimated using the conventional method during the off-pump condition.

MATERIALS AND METHODS

This study was performed in three healthy adult goats (female, 54, 52, and 58 kg) with the left ventricle assisted by the centrifugal pump NEDO PI-710 gyro pump (Baylor College of Medicine, Houston, TX, USA) in animals 1 and 2, and by the centrifugal pump EvaHeart (Sun Medical Technology Research Corporation, Nagano, Japan) in animal 3. The RBP outflow cannula was anastomosed to the descending aorta and the inflow cannula was inserted into the left ventricular apex. All animals received humane care in accordance with the guidelines determined by the Institutional Animal Care and Use Committee of Tohoku University. Ultrasonic flow meters (Transonic Systems, Inc., Ithaca, NY, USA) were placed on the pump outflow cannula and on the ascending aorta. A conductance catheter (Leycom, The Netherlands) was inserted into the left ventricle through the ascending aorta for continuous monitoring of the left ventricular pressure (LVP) and volume (LVV). Pump rotational speed and motor power supply were monitored through the controller. Heart failure conditions were mimicked by the injection of propranolol. The drug dose was determined according to the animal's condition at the time of the injection (respectively, 1.7, 0.25, and 2 mg). Each data set was recorded for 60 s with constant mean rotational speed at a sampling frequency of 1 kHz, starting at least 60 s after any changes in the rotational speed for the stabilization. For each animal, 12 data sets were recorded: six sets recorded at the control condition (hereinafter referred to as normal cardiac function [NCF]) and six sets recorded after the propranolol injection (hereinafter referred to as low cardiac function [LCF]); at each cardiac condition, one set was recorded with the pump stopped and the outflow cannula clamped, while the other five sets were recorded each one with a different mean pump rotational speed. The data with the pump stopped was recorded during manual clamp of the aorta, which changed the ventricular afterload. This data was used for the estimation of E_{max} using the multiple-beats method, approximating the E_{max} to the end-systolic elastance (E_{ES}), which corresponds to the slope of the end systolic pressure volume relationship (ESPVR) (2-4). The other data were used for the estimation of E_{max} using the POM, a method in which the E_{max} is estimated at each cardiac cycle independent of changes in the ventricular load. This method consid-